Journal of Hazardous Materials 453 (2023) 131432

Contents lists available at ScienceDirect

Journal of Hazardous Materials

journal homepage: www.elsevier.com/locate/jhazmat

The influences of dissolved inorganic and organic phosphorus on arsenate toxicity in marine diatom *Skeletonema costatum* and dinoflagellate *Amphidinium carterae*

Qunhuan Ma [a,b], Li Zhang [a,*]

[a] Key Laboratory of Tropical Marine Bio-resources and Ecology, Guangdong Provincial Key Laboratory of Applied Marine Biology, South China Sea Institute of Oceanology, Chinese Academy of Sciences, Guangzhou 510301, China
[b] University of Chinese Academy of Sciences, Beijing 100049, China

HIGHLIGHTS

- As(V) is more toxic to marine microalgae in DOP culture than in DIP culture.
- As(V) uptake and accumulation are higher in marine microalgae in DOP than in DIP.
- As(V) is biotransformed to organic As species in *S. costatum* but not in *A. carterae*.
- *carterae* increases the ratio of As(III) to As(V) in seawater.

GRAPHICAL ABSTRACT

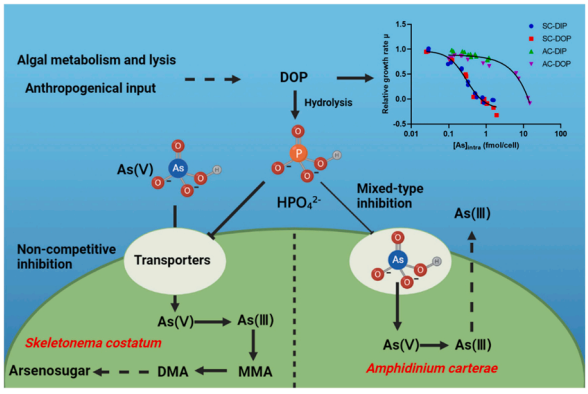

ARTICLE INFO

Editor: Baiyu Zhang

Keywords:
Arsenate
Marine microalgae
Dissolved organic phosphorus
Bioaccumulation
Biotransformation

ABSTRACT

In this study, arsenate (As(V)) uptake, bioaccumulation, subcellular distribution and biotransformation were assessed in the marine diatom *Skeletonema costatum* and dinoflagellate *Amphidinium carterae* cultured in dissolved inorganic phosphorus (DIP) and dissolved organic phosphorus (DOP). The results of 3-days As(V) exposure showed that As(V) was more toxic in DOP cultures than in DIP counterparts. The higher As accumulation contributed to more severe As(V) toxicity. The 4-h As(V) uptake kinetics followed Michaelis–Menten kinetics. The maximum uptake rates were higher in DOP cultures than those in DIP counterparts. After P addition, the half-saturation constants remained constant in *S. costatum* (2.42–3.07 μM) but decreased in *A. carterae* (from 10.9 to 3.8 μM) compared with that in the respective P-depleted counterparts. During long-term As(V) exposure, *A. carterae* accumulated more As than *S. costatum*. Simultaneously, As(V) was reduced and transformed into organic As species in DIP-cultured *S. costatum*, which was severely inhibited in their DOP counterparts. Only As (V) reduction occurred in *A. carterae*. Overall, this study demonstrated species-specific effects of DOP on As(V)

* Corresponding author.
E-mail address: zhangli@scsio.ac.cn (L. Zhang).

https://doi.org/10.1016/j.jhazmat.2023.131432
Received 16 February 2023; Received in revised form 5 April 2023; Accepted 15 April 2023
Available online 17 April 2023

toxicity, and thus provide a new insight into the relationship between As contamination and eutrophication on the basis of marine microalgae.

1. Introduction

Arsenic (As), a carcinogenic pollutant, is widely distributed in aquatic systems, and recently As contamination has become a global environmental problem affecting more than 115 countries [17]. The biological conversion of arsenate (As(V)) to arsenite (As(III)) is impaired in eutrophic lakes, suggesting the relationship between phosphorus (P) and As metabolism in resident microalgae [11,36]. The eutrophic process in coastal seawater has accelerated in recent years, and the increased anthropogenic input of dissolved organic phosphorus (DOP) is a major concern [13]. The increased ratio of DOP to dissolved inorganic phosphorus (DIP) in eutrophic areas is regarded as a critical driver in microalgae community succession, where the dominant species is changed from diatoms to dinoflagellates [32]. Diverse P strategies facilitate the dominance of diatoms and dinoflagellates in ecosystems with different P compositions [23]. As and P belong to the same group in the periodical table and share similar physiochemical properties [43]. The coexistence of As in the P minerals indicates the potential As contamination in the industrial and agricultural production [8]. Drainage from nearshore P fertilizer production inputted large amounts of As into eutrophic estuary, revealing the close relationship among As, eutrophic P and the resident microalgae [14]. Previous studies show that As uptake, accumulation, and metabolism in microalgae are influenced by P, and As toxicity are various among different microalgae species [17, 34,5]. Therefore, it is reasonable that the succession of dominant microalgae species influenced by DIP and DOP might alter the fate of As.

In seawater, DIP, the preferential P source, can be directly absorbed and assimilated by microalgae [32]. Previous studies have investigated the effects of DIP on As toxicity in microalgae. The increase in DIP concentration alleviates As toxicity in green alga, cyanobacteria, diatoms and dinoflagellates [15,49,54]. It has been widely accepted that As uptake is primarily via phosphate transporters, and uptake is impaired at elevated DIP concentrations [9]. Once it enters the cells, As is distributed in different subcellular fractions, chelated with sulfur-containing compounds, and transformed into diverse As species, the processes of which are correlated with DIP concentrations and alter As toxicity [47].

DOP contains various chemical forms and is primarily composed of nucleic acids, phospholipids, phosphorylated proteins, and sugars released by plankton production and anthropogenic activities [55]. High DOP concentrations, sometimes in excess of DIP concentrations, can be detected in surface seawater; thus, DOP is a significant alternative P source in DIP-limited waters [25]. DOP containing phosphoesters (C-O-P bonds, e.g., adenosine triphosphate) is bioavailable for most microalgae including diatoms, green alga, dinoflagellates [3]. The extracellular hydrolysis of phosphoesters to release DIP is the most prevalent DOP utilization mechanism in marine microalgae and is advantageous to dinoflagellates in outcompeting diatoms [23]. Moreover, some dinoflagellates can directly utilize DOP through phagotrophy without extracellular hydrolysis [22]. Efficient DOP utilization facilitates dinoflagellates dominance at high ratios of DOP to DIP [31]. In contrast, diatoms with higher growth rates outcompete dinoflagellates when DIP is sufficient [33].

Therefore, this study hypothesized that DIP and DOP would have different influences on the As toxicity, and the influences would differentiate between diatoms and dinoflagellates. The diatom *Skeletonema costatum* and the dinoflagellate *Amphidinium carterae*, two common and globally distributed species in coastal seawater, were used as the experimental species. Adenosine triphosphate (ATP, containing phosphoesters) was used as the representative DOP in this study, which is one of the ubiquitous DOP species in seawater and could be utilized as sole P source in diverse microalgae species [22,50,59]. Hydrolysis is the prevalent mechanism for ATP utilization and all the three P can be released via a series of phosphatases [16]. We conducted three series of experiments: 1) a three-day As(V) exposure experiment at DIP and DOP to analyze As(V) toxicity and accumulation; 2) a short-term As(V) exposure experiment (4 h) to reveal the As(V) uptake kinetic mechanisms; 3) a long-term As(V) exposure experiment (13 or 22 days) to examine the variation of As subcellular distribution and biotransformation.

2. Materials and methods

2.1. Algal culture

S. costatum was obtained from the Research Center of Harmful Algae and Marine Biology and Key Laboratory of Eutrophication and Red Tide Prevention of Guangdong Higher Education Institutes, Jinan University, China, and *A. carterae* was received from Key Laboratory of Tropical Marine Bio-resources and Ecology, South China Sea Institute of Oceanology, Chinese Academy of Sciences, China. Both algal species were maintained as a single strain and had been used in previous studies [27, 28]. *S. costatum* was cylindrical in shape with an estimated volume of 62 μm^3 [7]; whereas for oval-shaped *A. carterae*, the volume was approximately 297 μm^3 [46]. Aquil recipes were applied to all seawater preparations in this study [35]. Both algal species were cultured in f/2 medium [10], which was refreshed regularly to maintain the cells in a mid-exponential growth phase. As-free controls based on f/2 medium without As addition were applied in all the following experiments, and the tested medium As concentrations were below detection limit.

The chemicals used in seawater and medium preparation, except for vitamins and adenosine 5′-triphosphate disodium (5′-ATP-Na_2), were obtained from Guangzhou Chemical Reagent Factory (AR, China). Vitamin B_{12}, biotin and vitamin B_1 were obtained from Aladdin (China). All solutions were prepared using double deionized water (Milli-Q Millipore 18.2 MΩ·cm resistivity). The temperature was maintained at 22 ± 1 °C. The light intensity was 70 μmol photons/m^2/s with a 14:10 light-dark cycle. The medium pH and Eh were all analyzed at the beginning and the end of each experiment (pH: 7.95–8.02, Eh: 552–571 mV). The cultures were shaken twice daily to prevent cell sedimentation. A mixture of antibiotics, including kanamycin (50 mg/L), streptomycin sulfate (50 mg/L), and carbenicillin (100 mg/L), was added before the experiments to eliminate bacterial contamination [24].

Before transferring to different media, cells from different primary cultures were pre-treated in P-depleted conditions for three days to reach P deficiency. The initial cell density in the following experiments was approximately 2.5×10^5 cells/mL for *S. costatum* and 5×10^4 cells/mL for *A. carterae* because the carbon content in *S. costatum* was approximately one-fifth of that in *A. carterae*.

2.2. Three-day As(V) exposure

After P-depletion and twice sterile seawater washes, all treatments were transferred to different toxicity media (f/2 media without P addition as the basement). For both algal species, the DIP treatments contained 1.5 μM DIP (Na_2HPO_4) and DOP treatments contained 0.5 μM ATP (=1.5 μM-P) (5′-ATP-Na_2, Amresco, USA). The P concentration was referred to that in eutrophic coastal seawater [29]. SC-DIP and SC-DOP was the abbreviation for *S. costatum* cultured in DIP and DOP, respectively; Similarly, AC-DIP and AC-DOP represented *A. carterae* cultured in DIP and DOP, respectively. As(V), the dominant As species in aerobic seawater, is selected in this study and medium As(V) concentrations

($[As]_{medium}$) were 0.1, 0.2, 0.3, 0.4, 0.8, 4, and 10 μM ($Na_2HAsO_4{\cdot}7\ H_2O$, Sigma, USA). The As(V) concentrations in the range of 0.1–0.8 μM were relevant to those in coastal seawater covering natural and polluted conditions [14,30]. The two relatively high As(V) concentrations (4 and 10 μM) were set to obtain an entire dose response in SC-DIP, SC-DOP and AC-DOP. However, for AC-DIP, much higher As(V) concentrations (50, 100, and 200 μM) should be applied to reach the entire growth inhibition. Duplicates were applied in all treatments, and the media were prepared 24 h in advance for pre-equilibrium. Water filtrated through a 0.45 μm polyether sulfone filter was used in all media and was sampled at the beginning of the experiment. The total As content in the media was analyzed, and the actual As concentration was 91–98% of the nominal As(V) concentration.

The sampling time points were 24 h, 48 h, and 72 h after exposure. At each time point, the cultures were collected by filtration, fixed in 2% Lugol's solution, and counted under a light microscope (UB102i, UOP, China) [56]. The specific growth rates were calculated as μ_s, where N_1 and N_2 denoted the cell densities at times t_1 and t_2, respectively.

$$\mu_s=(\log N_2-\log N_1)/(t_2-t_1) \quad (1)$$

To minimize the effect of P forms on cell growth, the relative growth rates (μ) were calculated by normalizing μ_s to the control (μ_0) ($\mu = \mu_s/\mu_0$). μ was used as the biological response to estimate the As(V) toxicity. The half-maximal effective concentration (EC50) based on the medium As(V) concentration was predicted using the following function:

$$BR = BR_{min} + \frac{BR_{max} - BR_{min}}{1 + 10^{(\log EC50 - BR)\times Hillslope}} \quad (2)$$

where BR was the biological response; BR_{max} and BR_{min} were the maximal and minimal biological responses, respectively; and EC50 was the concentration of 50% inhibition of μ. The hillslope was a slope factor reflecting the steepness of the curve. Meanwhile, a 15 mL aliquot of each replicate was collected and filtered onto a GF/C membrane (0.7 μm pore size, Whatman). Weakly adsorbed As on the cell surface was removed by phosphate buffer (0.1 M in f/2 medium, 30‰ salinity to maintain osmotic balance) modified from the method of Levy et al. [21]. The samples, which were washed following the order of sterile seawater, phosphate buffer, and subsequently sterile seawater, were prepared for intracellular As content ($[As]_{intra}$) and P content ($[P]_{intra}$) analyses. The $[As]_{intra}$ and $[P]_{intra}$ values of AC-DIP at the three extremely high As(V) concentrations were not used in the comparison but listed in Table S1.

2.3. Short-term (4 h) As(V) uptake kinetics

Both algal species were subjected to three groups of P treatments (P-depleted, DIP-, and DOP-treatments), and each group had two replicates. After P depletion, algae were sterilely transferred to uptake media containing 0.2, 0.6, 0.8, 2, 5, and 10 μM As(V). The DIP and DOP additions were the same as those in the three-day As(V) exposure. The experiment lasted for 4 h, with four sampling time points: 1 h, 2 h, 3 h, and 4 h. At each point, 15 mL aliquots were collected in duplicate for As analysis after washing with sterile seawater and phosphate buffer.

The uptake rates were calculated from the slope of the regression function of $[As]_{intra}$ versus time, which were hyperbolically correlated to $[As]_{medium}$ and their relationship was fitted into the Michaelis–Menten equation:

$$V = \frac{V_{max} \times [As]_{medium}}{K_d + [As]_{medium}} \quad (3)$$

where V_{max} (fmol/cell/h) was the maximum uptake rate, and K_d (μM) was the half-saturation constant, represented as the medium As(V) concentration when the uptake rate was half of V_{max}.

2.4. Long-term As(V) exposure

P-depleted algae were sterilely transferred to the exposure media based on f/2 recipes without P addition. Both algal species had DIP and DOP treatments similar to those of the three-day As(V) exposure. The $[As]_{medium}$ (0.6 μM) was close to the As concentration in polluted coastal waters [14]. Algae-free controls were set to investigate possible abiotic As transformation and 97–99% of the medium As species was still As(V) at the end of the experiment. Daily addition (1.5 μM-DIP or 0.5 μM-DOP) was performed to maintain cell survival during long-term exposure. The daily cell density was measured in the same manner as that in the three-day As(V) exposure experiment. The total exposure duration depended on the time to enter the stationary phase, which was obtained from preliminary experiments and was approximately 13 days and 22 days for *S. costatum* and *A. carterae*, respectively. Then, sampling time for *S. costatum* was Day 2, Day 6, and Day 13, representing the initial, medium, and final stages, respectively. The sampling time for *A. carterae* was Day 2 (initial stage), Day 6 and Day 13 (medium stages), and Day 22 (final stage). At each sampling time, medium P concentrations were measured before daily P addition and data were listed in Table S2. Similarly, 15 mL aliquots were collected in duplicate for As analysis.

At each stage, algae were collected in duplicate by centrifugation (5000 ×*g*, 15 min, 20 °C). After once phosphate buffer and twice sterile seawater washes, the cells were collected and disrupted using a high-pressure cell crusher (JN-Mini, JNBIO, China). The breakage efficiency was approximately 100%, as verified via microscopic examination. The separation process was maintained at 4 °C to prevent possible protein denaturation. The homogenate and the separated fractions were stored at − 80 °C for As analyses. In total, five cell fractions were separated, including heat-stable proteins (HSP: glutathione, phytochelatins and metallothioneins), cell debris (CD: cell walls and residue of cells), organelles (mitochondria, Golgi apparatus and endoplasmic reticulum), metal-rich granules (MRG: minerals, NaOH-resistant materials) and heat-denaturable proteins (HDP: enzymes). Furthermore, HSP and MRG were combined as biologically detoxified fractions (BDM), whereas HDP and organelles were combined as metal-sensitive fractions (MSF), as described by Wallace et al. [44]. The protocol for separating the subcellular fractions was modified from that described by Cremazy et al. [4], and the details were provided in the supporting materials.

2.5. Total As, P, and As species analysis

Samples collected in the filters were digested with 1 mL concentrated HNO_3 (70%, ultrapure, Fisher Scientific, Geel, Belgium). After heating at 80 °C for 24 h, the clear digested liquid was diluted with double-deionized water for later analysis. The water samples were acidified to 1% HNO_3 in a proper volume. Blank sample preparation was performed following the same procedure. Total As analyses using an inductively coupled plasma mass spectrometer (PerkinElmer NexION 350X, Germany) followed the modified methods of Zhang et al. [58]. ^{72}Ge was used as the internal standard of As to correct the sensitivity drift and matrix effects. The accuracies of As were testified by the certified reference material of mussels (GBW08571), and measured values for total As was 103.3% (6.3 ± 1.2 μg/g) of the certified value. Standard solutions of As (NSI Lab Solutions, USA) were prepared from stock solutions. The recovery rate of As was 90–110%. The P content was measured using a modified molybdenum-antimony spectrophotometric method [52].

As species were analyzed according to the modified method of Xue et al. [53]. The homogenate was filtered through a 0.22-μm filters (polyether sulfone, Jinteng, China) and As species analysis was carried out using a PerkinElmer NexION 350X ICP-MS coupled with a Waters HPLC system (Waters 2707 autosampler and Waters 1515 Isocratic HPLC Pump; Waters, U.S.A). PRP-X100 with a guard column was applied for separation (Hamilton, Reno, NV, U.S.A.) and

chromatography parameters were listed in Table S3. BCR-627 Tune Fish Tissue (Institute for Reference Materials and Measurements, Geel, Belgium) was used to assess the accuracy and the recovery was 89.7–98.4% for arsenobetaine (AsB), 83.5–97.3% for dimethylarsenic acid (DMA), 81.9–92.1% for As(V), 90.2–96.5% for monomethylarsenic acid (MMA), and 80.6–94.7% for As(III).

2.6. Statistical analysis

Two-way analysis of variance followed by Tukey's test was applied to determine significant differences in SPSS 20.0. Regression analysis and figure preparation were conducted using GraphPad Prism 9 software. Differences were considered significant at a probability level of less than 0.05.

3. Results

3.1. Algal toxicity of As(V)

Our preliminary study showed that both algal species could utilize ATP as their sole P source (Fig. S1). Although the growth of DOP-cultured *S. costatum* was obviously slowed down from Day 4, the growth of DOP-cultured *A. carterae* was similar to that of their DIP counterparts, indicating better DOP utilization in *A. carterae*.

The As(V) toxicity was determined by inhibition of cell growth. In both forms of P, As(V) toxicity was more severe in *S. costatum* than in *A. carterae* (Fig. 1 and S2). Obvious growth retardance was exhibited in As(V) concentrations > 0.3 μM for *S. costatum*, whereas the growth was still maintained in 4 μM-As(V) for *A. carterae*. Accordingly, EC50s were 0.305 and 0.291 μM for SC-DIP and SC-DOP, respectively, which were much lower than those in *A. carterae* (61.8 and 4.06 μM for AC-DIP and AC-DOP, respectively). As(V) toxicity was also P-form-dependent, with more severe As(V) toxicity exhibited in DOP cultures than in their respective DIP counterparts, although this was not obvious in *S. costatum*. However, EC50 in AC-DIP was 15-fold higher than that in AC-DOP. Therefore, the regression curves describing the relationship between the $[As]_{medium}$ and μ were diverse, depending on P forms in both algal species (Fig. 2B).

S. costatum and *A. carterae* accumulated 0.03–1.74 fmol/cell and 0.1–13.9 fmol/cell As at respective $[As]_{medium}$. Generally, $[As]_{intra}$ increased and then reached saturation at elevated $[As]_{medium}$ except for AC-DOP (Fig. 2A). The $[As]_{intra}$ in *A. carterae* was more than 4-fold higher than *S. costatum* under the lowest As(V) exposure (0.1 μM-As (V)). Higher As accumulation was observed in DOP cultures in both species, more than 12-fold higher for *A. carterae* and less than 2-fold higher for *S. costatum* at the highest $[As]_{medium}$. μ correlated well with $[As]_{intra}$ in both algal species, covering all As and P combinations (Fig. 2C).

Compared with $[P]_{intra}$ in *S. costatum* (19.2–78.4 fmol/cell), higher $[P]_{intra}$ in *A. carterae* (127–284 fmol/cell) contributed to the lower [As:P] in *A. carterae* (Fig. S3). Meanwhile, both species exhibited an increase in [As:P] in DOP cultures compared with that in their DIP counterparts. Similarly, the relationship between [As:P] and μ could be described by unified regression functions for both algal species (Fig. 2D).

3.2. Short-term As(V) uptake

$[As]_{intra}$ increased linearly with time during the 4 h As(V) exposure; therefore, the As(V) uptake rate was represented by the slope of each regression (Fig. S4). Higher uptake rates were observed in *A. carterae* (0.040–0.594 fmol/cell/h) than in *S. costatum* (0.035–0.202 fmol/cell/h) in their respective $[As]_{medium}$. Compared with respective DIP counterparts in both algal species, higher rates were exhibited in DOP cultures, although they only slightly increased in *S. costatum* (Fig. 3). The

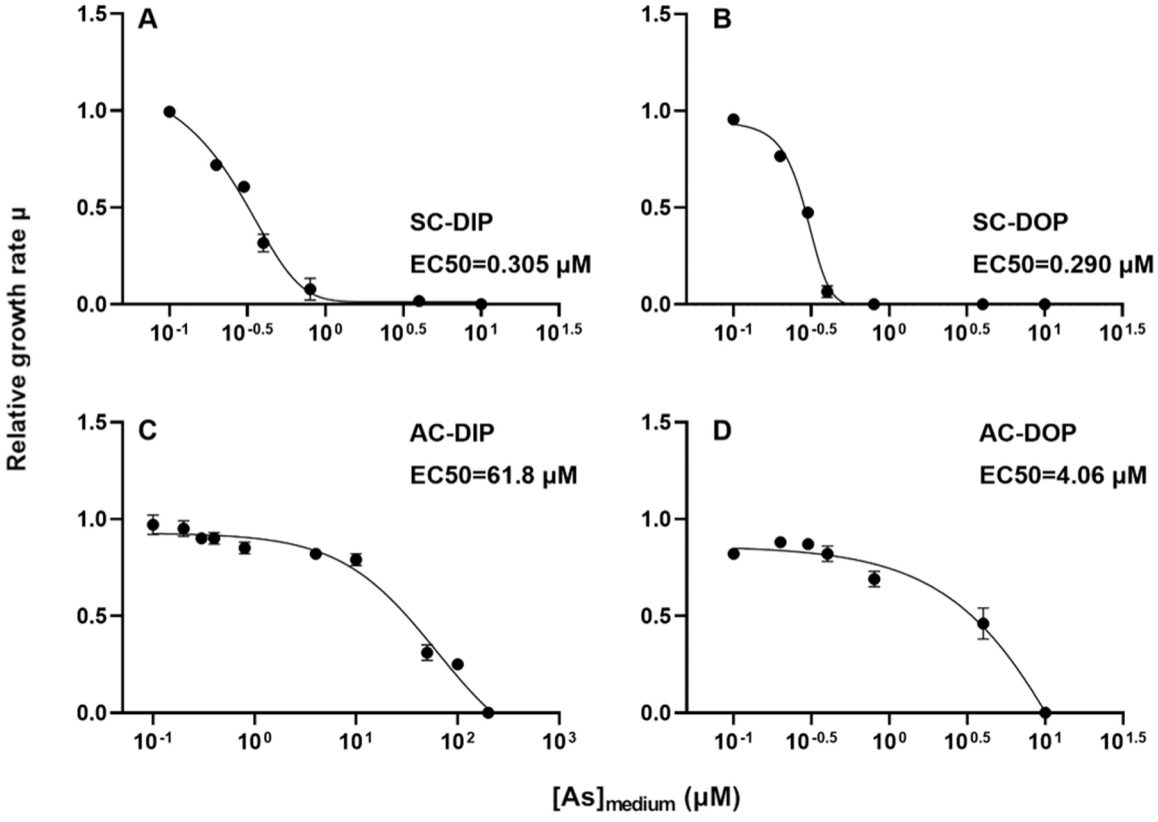

Fig. 1. Relative growth rates (μ) of *Skeletonema costatum* and *Amphidinium carterae* exposed to different medium As(V) concentrations ($[As]_{medium}$, μM) for three days. The half-maximal effective concentration (EC50) was shown in the panels. A and B represented *S. costatum* cultured in DIP and DOP; C and D represented *A. carterae* cultured in DIP and DOP. Data were mean ± standard deviation (n = 2).

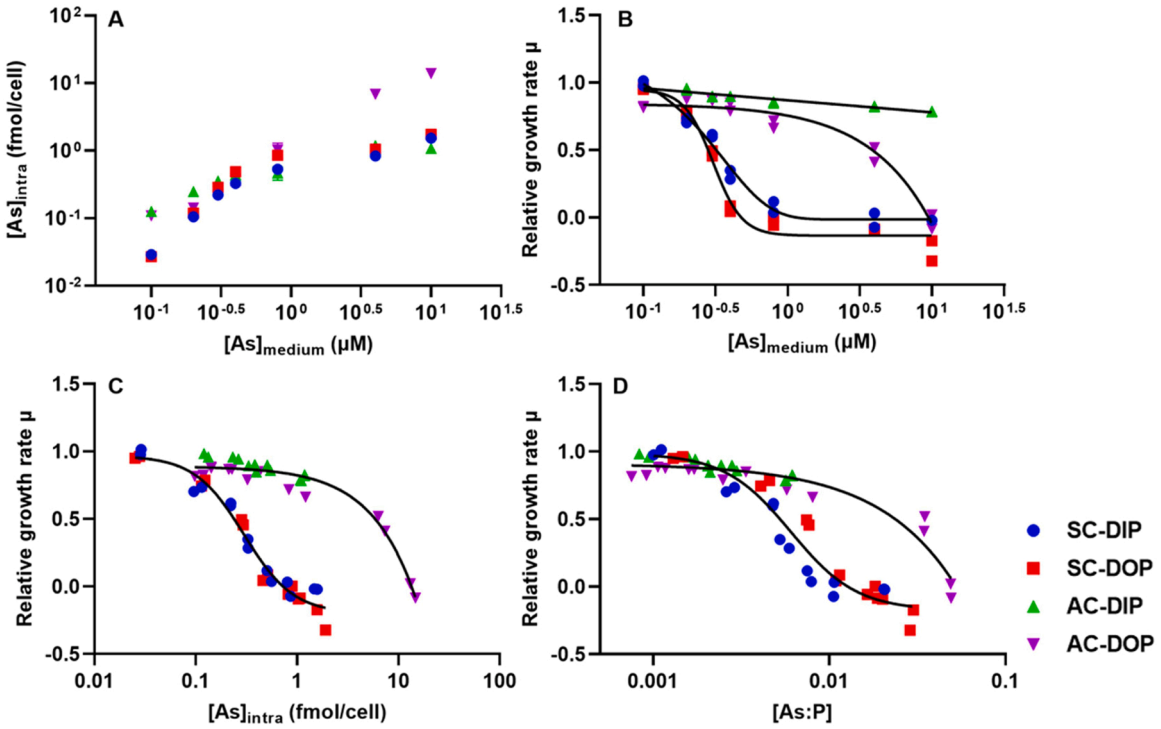

Fig. 2. Intracellular arsenic content ($[As]_{intra}$, fmol/cell; A) and the correlations of the relative growth rates (μ) to either $[As]_{medium}$ (B), $[As]_{intra}$ (C), or the ratio of intracellular As to P ([As:P]; D) of *Skeletonema costatum* and *Amphidinium carterae* after three-day As(V) exposure. SC-DIP and SC-DOP represented *S. costatum* cultured in DIP and DOP. AC-DIP and AC-DOP represented *A. carterae* cultured in DIP and DOP. Logistic dose-response model and line regression function were applied to describe the correlation in *S. costatum* and *A. carterae*, respectively. Data were mean ± standard deviation (n = 2, most error bars are too small to shown) in panel A, while each point indicated the μ at respective $[As]_{medium}$ and P forms in panel B, C and D.

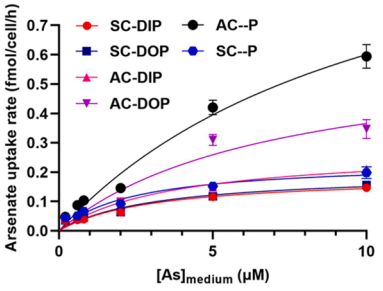

	V_{max} (fmol/cell/h)	K_d (μM)
SC--P	0.236	2.42
SC-DIP	0.188	3.04
SC-DOP	0.197	3.07
AC--P	1.25	10.9
AC-DIP	0.279	3.78
AC-DOP	0.622	7.00

Fig. 3. As(V) uptake rate (fmol/cell/h) at different $[As]_{medium}$ (μM) and uptake parameters in *Skeletonema costatum* and *Amphidinium carterae* obtained from Michaelis–Menten equation. V_{max} (fmol/cell/h): maximum As(V) uptake rate; K_d (μM): half-saturation constant. SC–P, SC-DIP and SC-DOP represented *S. costatum* cultured in P-depletion, DIP and DOP. AC–P, AC-DIP and AC-DOP represented *A. carterae* cultured in P-depletion, DIP and DOP. Solid lines were simulated by the Michaelis–Menten equation. The uptake parameters were shown in the panel. Data were mean ± standard deviation (n = 2).

hyperbolic correlation between the As(V) uptake rate and $[As]_{medium}$ could be fitted by Michaelis–Menten equation. The trends of V_{max} were similar to those of the As(V) uptake rate, while K_d was species-dependent. An approximately two-fold increase of K_d was observed in AC-DOP compared with that in AC-DIP; however, K_d was nearly no change in *S. costatum*.

Compared to the respective P-depletion treatments, V_{max} decreased after either DIP or DOP addition in both algal species. The K_d was almost constant in *S. costatum* (2.42–3.07 μM) while obviously declined in *A. carterae* (from 10.9 to 3.8 μM).

3.3. Long-term As(V) exposure

Similar to the three-day As(V) exposure, As(V) toxicity was exhibited by growth inhibition during long-term As(V) exposure, which was more severe in DOP treatments for both algal species compared with that in their DIP counterparts (Fig. 4A and B). Accordingly, more As was accumulated in the DOP treatments (Fig. 4C).

The subcellular distribution of As was both species-specific and P-form-dependent (Fig. 5). There was a time-scale change in *S. costatum* in which As was primarily distributed in BDM at the initial and medium stages (Day 2 and Day 6), and CD became the majority at the final stage (Day 13). In contrast, BDM was the major fraction of the As subcellular distribution in *A. carterae* during the entire exposure period. The forms of P had nearly no influence on As subcellular distribution in *A. carterae* but there was a significant increase in CD distribution in SC-DOP compared with that in SC-DIP at the final stage ($p < 0.05$).

In total, five As species (As(V), As(III), MMA, DMA and a phosphate arsenosugar-like species) were separated in this study (Fig. 6). However, methyl arsenic species (MMA and DMA) and arsenosugar-like species were only detected in SC-DIP. In contrast, the As transformation nearly disappeared in SC-DOP. For *A. carterae*, only the reduction of As(V) to As (III) occurred, which was slightly inhibited in AC-DOP. No organic As species were detected in the medium (Fig. 7). As(V) was the predominant As species in the medium of *S. costatum*, while the percentage of As (III) increased significantly in the medium of *A. carterae*.

4. Discussion

4.1. P-form-dependent As(V) toxicity

The influences of different P forms on As toxicity, uptake, accumulation, subcellular distribution and transformation were shown in *S. costatum* and *A. carterae*. The present study demonstrated that As(V)

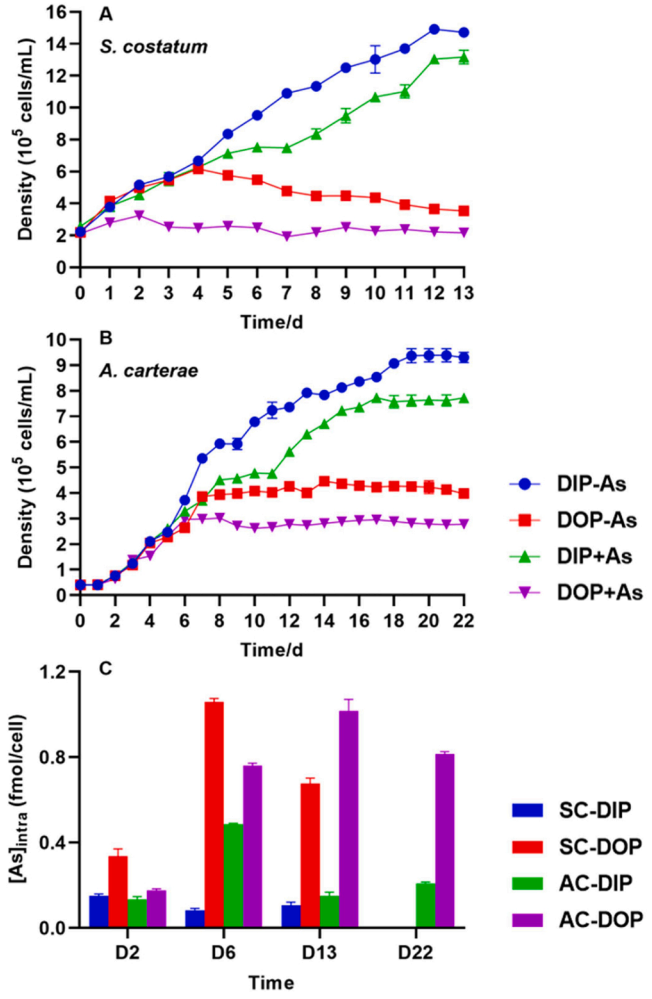

Fig. 4. The cell density (10^5 cells/mL) in *Skeletonema costatum* (A) and *Amphidinium carterae* (B), and $[As]_{intra}$ (C) during long-term As(V) exposure. In panel A and B, DIP-As and DOP-As represented DIP and DOP cultures without As(V) addition, and DIP + As and DOP + As represented DIP and DOP culture with 0.6 μM As(V) exposure. In panel C, SC-DIP and SC-DOP represented *S. costatum* cultured in DIP and DOP, and AC-DIP and AC-DOP represented *A. carterae* cultured in DIP and DOP. Data were mean ± standard deviation (n = 2).

inhibited algal growth in both forms of P. More severe As(V) toxicity was observed in AC-DOP than in AC-DIP, while it only slightly increased in SC-DOP (Fig. 1 and S2). The species-specific regression relationship between $[As]_{medium}$ and μ was in accordance with this discrepancy (Fig. 2B). Severe As(V) toxicity had also been exhibited in *Microcystis. aeruginosa* cultured in different types of DOP [50]. As(V) toxicity was diverse in previous studies, even for the same species [18,45]. Therefore, our study suggested that such discrepancies in As(V) toxicity might result from different medium P compositions; however, relevant data in previous studies were absent [1,21].

The present study demonstrated that $[As]_{intra}$ was well correlated to As(V) toxicity in different forms of P. Previous studies also demonstrated that $[As]_{intra}$ could indicate As(V) toxicity in *S. costatum* and the marine green algae *Chlorella salina* at different DIP conditions [19,27]. There was more As accumulated in AC-DOP especially at ambient As(V) concentrations > 0.8 μM, which was in accordance with the obvious decrease of EC50s. While a slight increase in $[As]_{intra}$ was observed in SC-DOP compared with that in SC-DIP, the EC50s of which were close (Figs. 1 and 2 A). Higher As accumulation in DOP cultures was also exhibited in short-term As(V) uptake and long-term As(V) exposure (Fig. 4 C and S4). As accumulation was regarded as misidentification under P stress, where the intracellular P shortage facilitated involuntary As uptake [41]. In this study, lower $[P]_{intra}$ was exhibited in SC-DOP and AC-DOP compared with that in respective DIP counterparts (Table S3, except for *A. carterae* in 4 and 10 μM-As(V)). The imbalance of intracellular As and P was shown by elevated [As:P] in DOP cultures (Fig. S3). The correlation of either $[As]_{intra}$ or [As:P] to cell growth could be fitted by unified functions in *S. costatum* and *A. carterae*, which suggested that $[As]_{intra}$ was the key contributor to the discrepancies of As(V) toxicity in different P forms (Fig. 2 C and D). Similarly, DOP-cultured *M. aeruginosa* with more severe As(V) toxicity exhibited an increase in $[As]_{intra}$ and [As:P] compared to those in their DIP counterparts [50].

The present study showed higher As(V) uptake rates in both DOP-cultured algal species (Fig. 3). Previous studies had rarely focused on the effects of different forms of P on As uptake. The ATP utilization was mainly through hydrolysis, and the breakage of three phosphoesters was catalyzed by a series of phosphatases [16]. The different efficiencies of ATP hydrolysis among diverse microalgae species were directly linked to P supply and subsequently influenced on the fate of As. For cyanobacteria in the oligotrophic North Pacific, an improvement in As resistance was correlated with good DOP utilization, which supplied more DIP to effectively inhibit As uptake [12]. As an analog of P, As(V) uptake was primarily via phosphate transporters [9]. The antagonistic effect of P on As(V) uptake was mainly through taking up the available transporters, and such inhibition was enhanced at elevated DIP concentrations, which had been verified in green alga, cyanobacteria, and diatoms [40,48,51]. In contrast, the inhibition of As(V) uptake by DOP could not function directly before hydrolysis. In other words, the inhibitive efficiency on As(V) uptake primarily depended on the amount of DIP supplied through DOP utilization. Similar to uptake rates, V_{max} (uptake parameter indicating the number of available transporters) was higher in DOP cultures. Therefore, we assumed that the incomplete utilization of DOP failed to provide equivalent P as their DIP counterparts, and thus, more transporters were available for AsV uptake.

In this study, the other key uptake parameter K_d (indicated the binding affinity to transporters) was nearly constant in SC-DOP and increased in AC-DOP compared with that in their DIP counterparts. Compared with respective P-depleted counterparts, K_d remained unchanged in *S. costatum* and decreased in *A. carterae* after P addition, suggesting different P inhibition mechanisms for As(V) uptake in the two species. In reversible inhibition mechanisms, the non-competitive inhibitor would not alter K_d (equal binding affinity) but would lower the value of V_{max} (decrease in the number of available transporters). In mixed-type inhibition, both V_{max} and K_d decreased [37]. The traits of V_{max} and K_d in this study indicated that P was a non-competitive inhibitor in *S. costatum* and a mixed-type inhibitor in *A. carterae* (Fig. 8). As a non-competitive inhibitor, P consumed the limited transporters instead of altering the binding affinity, and this effect was weaker in DOP cultures. In mixed-type inhibition, higher P-binding affinity of As-transporter complexes promoted more transporter-As-P complexes to be synthesized and drove As-uptake equilibrium toward the formation of As-transporter complexes, as shown by the decline in K_d values. The higher value of K_d in DOP-culture indicated the weaker effects of P on altering the binding affinity of As-transporter complexes, which might also result from the incomplete utilization of DOP.

The three-day As(V) exposure showed that $[As]_{intra}$ was similar among SC-DIP, SC-DOP, and AC-DIP, although As(V) toxicity was rather different (Fig. 2A). Therefore, apart from $[As]_{intra}$, the fate of internalized As(V) such as subcellular distribution and biotransformation, should also be considered. The present study showed that the percentage of CD was significantly increased in SC-DOP at the final stage. The CD fraction mainly consisted of cell walls and residue of cells [20]. The severe growth inhibition accompanying the higher percentage of CD in SC-DOP suggesting the increase of CD percentage resulted from cell mortality. In contrast, BDM was the major distribution in *A. carterae* during the entire exposure period and in *S. costatum* during the initial and medium stages. The subcellular distribution could indicate the

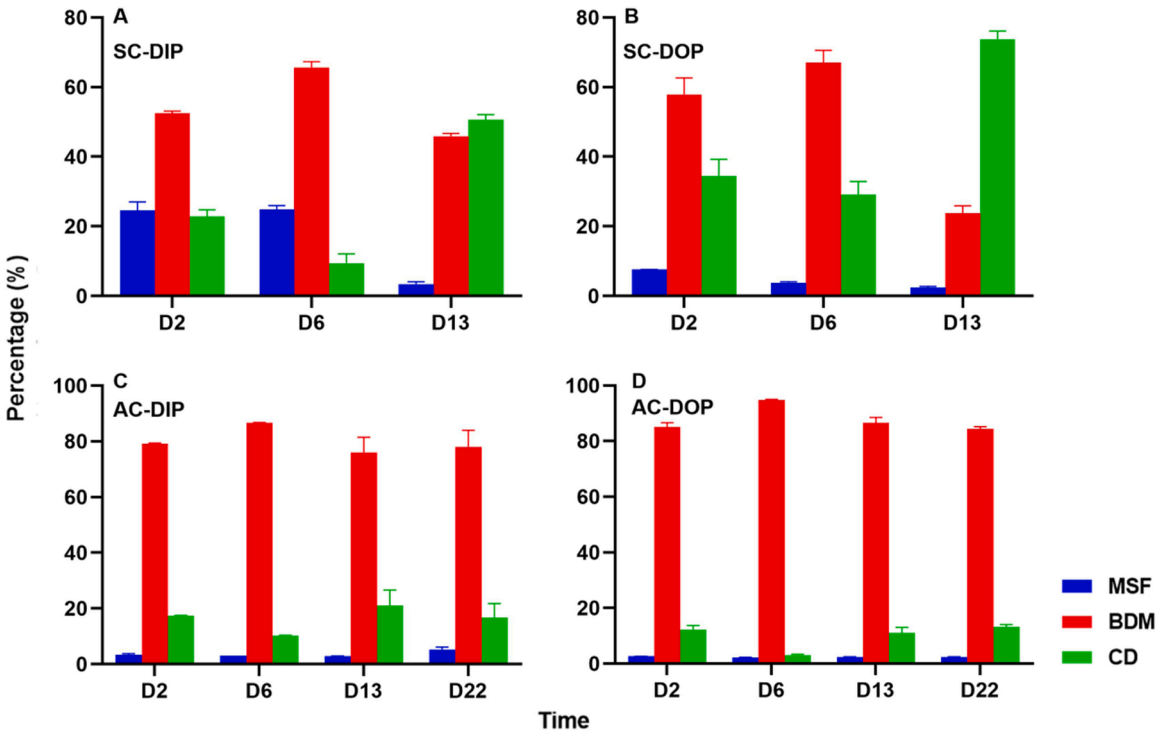

Fig. 5. Subcellular distribution of arsenic (As) in *Skeletonema costatum* and *Amphidinium carterae* during long-term As(V) exposure. A and B represented *S. costatum* cultured in DIP and DOP; C and D represented *A. carterae* cultured in DIP and DOP. Metal-sensitive fractions (MSF): heat-denatured proteins (HDP) and organelle; Biologically detoxified fractions (BDM): heat-stable proteins (HSP) and metal-rich granules (MRG); Cell debris (CD). Data were mean ± standard deviation (n = 2).

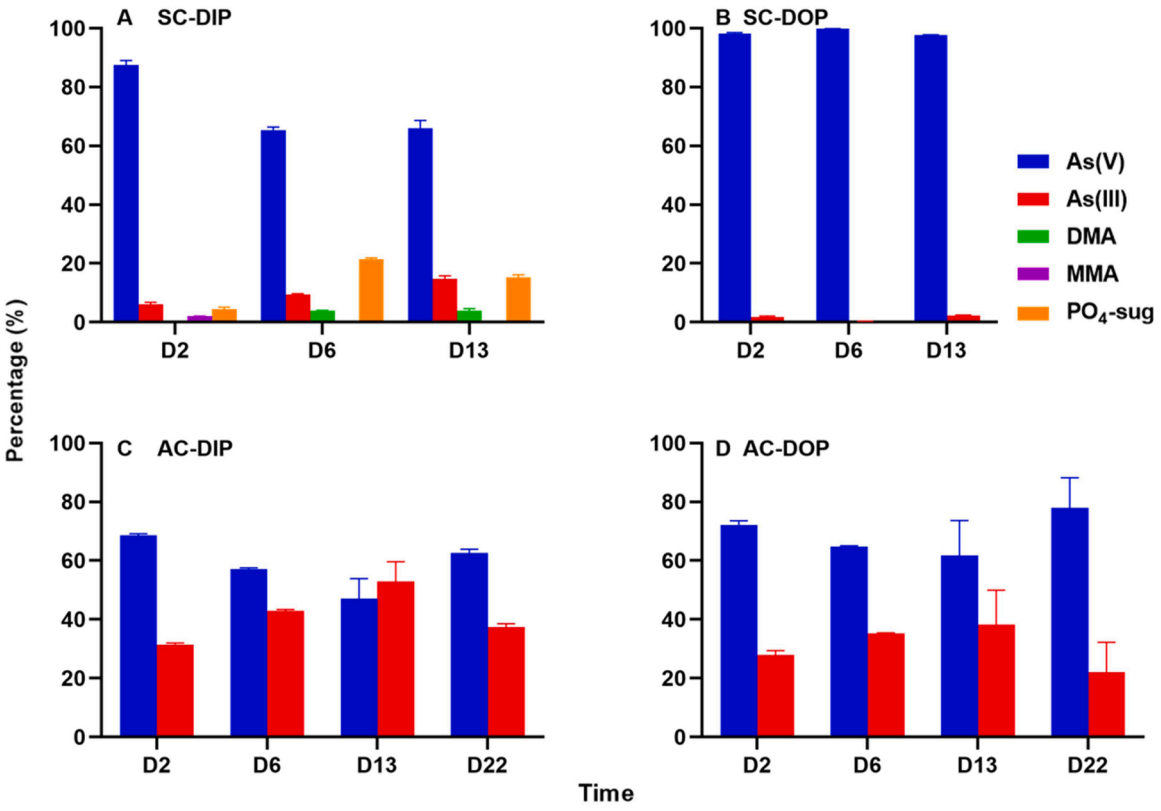

Fig. 6. The percentage of As species (As(V): arsenate; As(III): arsenite; MMA: monomethylarsenic acid; DMA: dimethylarsenic acid; PO_4-sug: phosphate arsenosugar-like species) in *Skeletonema costatum* and *Amphidinium carterae* during long-term As(V) exposure. Panel A and B represented *S. costatum* cultured in DIP and DOP, and panel C and D represented *A. carterae* cultured in DIP and DOP. Data were mean ± standard deviation (n = 2).

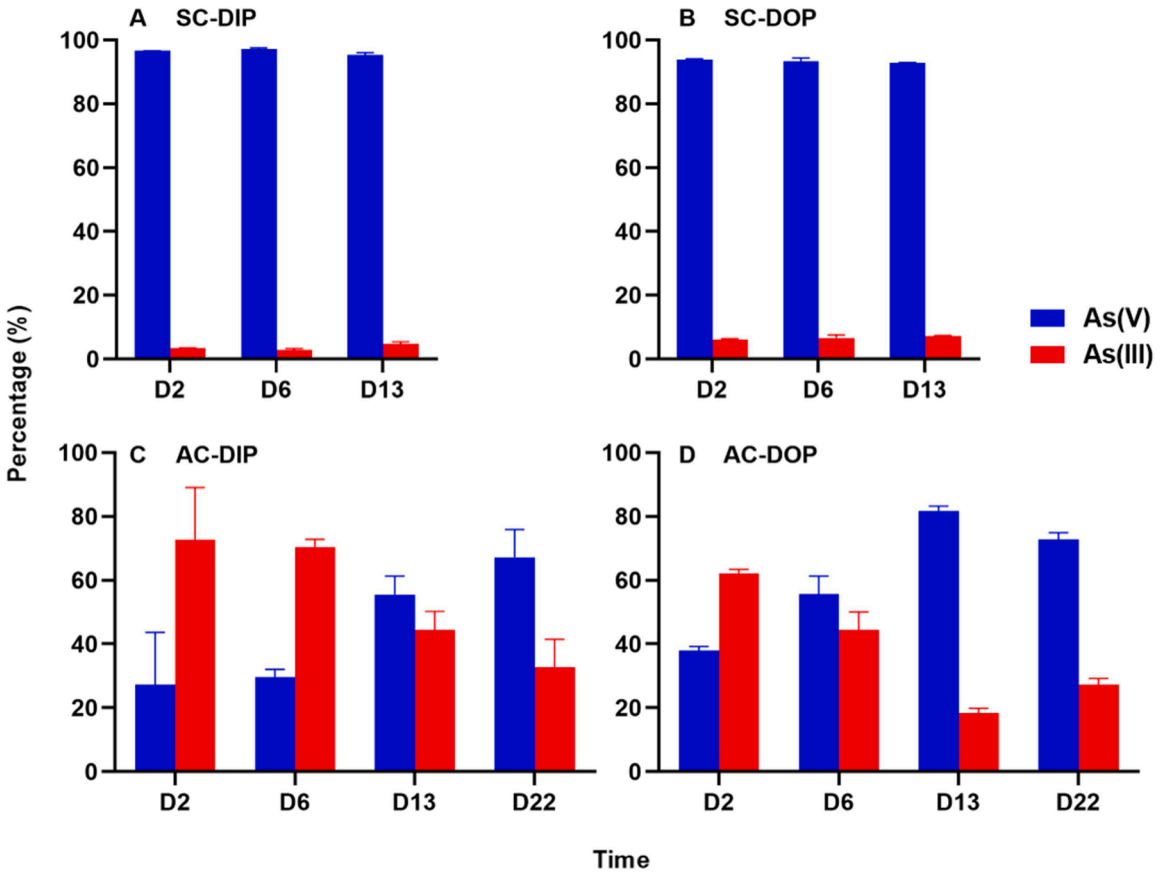

Fig. 7. The percentage of As(V) and As(III) in algae culture media during long-term As(V) exposure. Panel A and B represented *Skeletonema costatum* cultured in DIP and DOP, and panel C and D represented *Amphidinium carterae* cultured in DIP and DOP. Data were mean ± standard deviation (n = 2).

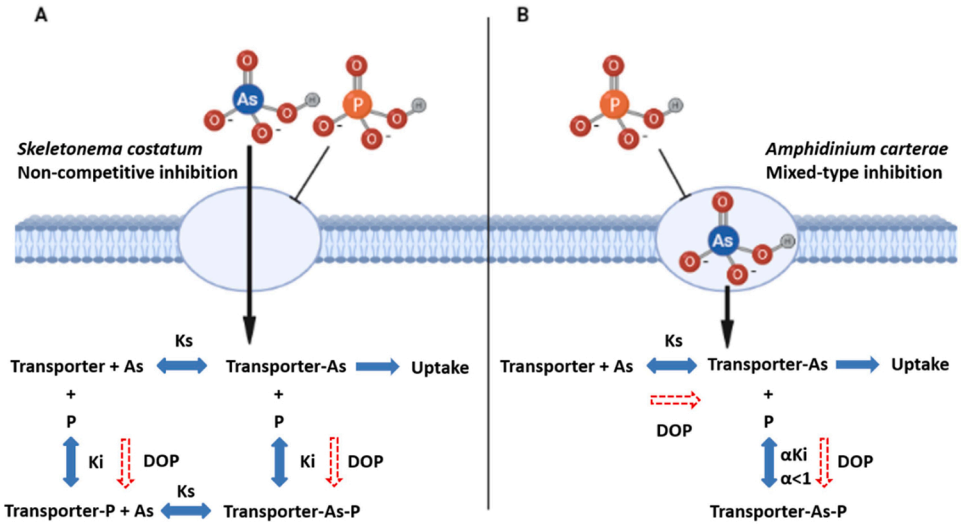

Fig. 8. Schemes of inhibitive effects of P on As (V) uptake in *Skeletonema costatum* (A) and *Amphidinium carterae* (B), respectively. Oval represented phosphate transporters. Ks and Ki represented the dissociation constant of transporter-As complexes and transporter-P complexes, respectively. α is the coefficient for the variation of Ki. The blue bidirectional arrows indicated the reversible equilibriums. The red dash arrows pointed out the weaker effects of DOP on altering direction compared with DIP counterparts.

internal mechanisms of metal accumulation, and the percentages of different fractions reflected metal toxicity and tolerance [44]. The distribution in BDM was regarded as a detoxification process, indicating metal tolerance and resistance [2,38]. However, distribution in MSF was linked to metal toxicity [44]. Subcellular distribution under the effects of different forms of P in microalgae had rarely been investigated, except for *M. aeruginosa*, where the major subcellular distribution was CD in DOP cultures and BDM in DIP counterparts [50]. Therefore, our study demonstrated that As distributed in BDM for detoxification could also function in *S. costatum* and *A. carterae*.

In the present study, As biotransformation was inhibited in SC-DOP. In contrast, reduction, methylation, and even complex organic As speciation synthesis occurred in SC-DIP (Fig. 6). The possible synthesis of phosphate arsenosugar-like species referred to Xue et al. [53] (Fig. S5). The toxicities of diverse As species had been ranked following the well-accepted order of: As(III) > As(V) > (MMA~DMA) > Complex organic As compounds (e.g. AsB, arsenocholine, and arsenosugars) [47]. The transformation of As speciation, which was of great significance in

algal detoxification, was under the influence of ambient DIP concentrations [6,57]. However, few studies had investigated whether different forms of P would affect the As biotransformation. In *M. aeruginosa*, reduction and methylation were promoted under DOP culture, which was the critical step in As detoxification [50]. Similarly, our study demonstrated that As reduction and subsequent methylation as the As detoxification mechanism also functioned in *S. costatum*; however, its efficiency was severely impaired in their DOP cultures.

4.2. Species-specific As(V) toxicity

In this study, As(V) toxicity was more severe in *S. costatum* than in *A. carterae*, suggesting the mechanisms of As(V) toxicity were species-specific. As(V) could be more quickly absorbed by *A. carterae* compared with that by *S. costatum* (Fig. 3). Accordingly, more As was accumulated intracellularly in *A. carterae* (Fig. S4). The higher As(V) uptake rates and $[As]_{intra}$ suggested *A. carterae* could uptake and accumulate large amounts of As in a short time. Moreover, the AC-DOP exhibited unlimited As accumulation under high levels of As(V) exposure (4 and 10 μM-As(V)). The possible phagotrophy for DOP (one of the representative P strategies for dinoflagellates [23]) accompanying unintentional As absorption might be one of the culprits. This dinoflagellate-specific ATP utilization mechanism might also explain the weaker inhibition of DOP during As(V) uptake, as the absorption of As through phagotrophy could not be alleviated by P-mediated uptake inhibition. In contrast, phagotrophy in diatoms, the tough cell wall of which consisted large amount of silica, had not been reported yet [26,42]. The absent phagotrophy for *S. costatum* might result in the similar inhibitive efficiency of P in SC-DIP and SC-DOP.

The internalized As(V) in *A. carterae* was primarily distributed in BDM, the process which could efficiently alleviate As(V) toxicity. Meanwhile, As(V) was reduced to more toxic As(III) in *A. carterae*. To alleviate toxicity, As(III) would be excreted or used as a substrate for further methylation and complex organic As species synthesis [5]. In this study, no methylated or complex organic As species were detected in the inner *A. carterae*. Instead, an obvious increase in As(III) was observed in the medium, which could exceed to As(V) (Fig. 7). The slower conversion of As(III) to organic As species, as well as quick As(III) exudation, might explain the absence of organic As species in *A. carterae*. The reduction and subsequent excretion for detoxification had been proven in marine microalgae, although it might increase As(III) ratio in seawater and thus unintentionally increase As risks [12]. The highest concentrations of As(III) accompanying phytoplankton blooms in the Patuxent River Estuary suggested that resident microalgae could indeed change the composition of As speciation in ambient seawater [39]. Differentially, the internalized As(V) in *S. costatum* was reduced and further synthesized to methylated and complex organic As species. However, this detoxified As(V) biotransformation was significantly impaired in SC-DOP.

In summary, our study revealed the potential risks of As at an elevated DOP condition. Compared with their DIP counterparts, higher $[As]_{intra}$ and [As:P] in DOP cultures contributed to more severe As toxicity. The microalgae community composition was gradually changed from diatom-dominance to dinoflagellate-dominance with an increase in the DOP/DIP ratio [23]. In the present study, dinoflagellate *A. carterae* uptake As quickly and subsequently accumulated As in a short time. Possible DOP phagotrophy enabled *A. carterae* to absorb more As unintentionally. The internalized As(V) after reduction was primarily excreted, thus elevating the ratio of As(III) to As(V) in ambient seawater. In contrast, the detoxified As biotransformation was severely impaired in diatom *S. costatum* in DOP cultures, and thus, more toxic inorganic As following the transfer from BDM to CD would possibly be released to the environment. Since diatoms flourished in DIP-sufficient eutrophic areas, their decay with the consumption of DIP and the anthropogenic input of DOP increased the DOP/DIP ratio under eutrophication. Therefore, attention should be paid to the ecological As risks when As pollution and eutrophication coexisted.

Environmental implication

The co-existence of arsenic (As) pollution and eutrophication is common in many coastal and estuarine environment. How the elevated dissolved organic phosphorus (DOP) affects As toxicity in marine microalgae is not clear yet. This study demonstrated As exhibited higher toxicity to marine diatoms and dinoflagellates in the presence of DOP than that of DIP by increasing the As uptake and accumulation. Dinoflagellates, the DOP consumer, elevated the ratio of high toxic arsenite in seawater. The DOP-cultured diatoms reduced their ability to transform toxic As to less toxic species. Therefore, DOP elevates the risks of As toxicity in eutrophic seawater.

CRediT authorship contribution statement

Qunhuan Ma: Methodology, Software, Formal analysis, Investigation, Resources, Writing – original draft preparation and revision, Visualization. **Li Zhang:** Conceptualization, Writing – review & editing, Supervision, Project administration, Funding acquisition.

Declaration of Competing Interest

The authors declare that they have no known competing financial interests or personal relationships that could have appeared to influence the work reported in this paper.

Data Availability

No data was used for the research described in the article.

Acknowledgement

This research was financially supported by the National Natural Science Foundation of China (41922042, 41876133, 41906137), Science and Technology Planning Project of Guangdong Province, China (2020B1212060058).

Appendix A. Supporting information

Supplementary data associated with this article can be found in the online version at doi:10.1016/j.jhazmat.2023.131432.

References

[1] Baker, J., Wallschlager, D., 2016. The role of phosphorus in the metabolism of arsenate by a freshwater green alga, *Chlorella vulgaris*. J Environ Sci 49, 169–178.
[2] Brown, B.E., 1982. The form and function of metal-containing granules in invertebrate tissues. Biol Rev Camb Philos Soc 57, 621–667.
[3] Cembella, A.D., Antia, N.J., Harrison, P.J., 1984. The utilization of inorganic and organic phosphorous compounds as nutrients by eukaryotic microalgae: a multidisciplinary perspective: Part 1. Crit Rev Microbiol 10, 317–391.
[4] Cremazy, A., Levy, J.L., Campbell, P.G., Fortin, C., 2013. Uptake and subcellular partitioning of trivalent metals in a green alga: comparison between Al and Sc. Biometals 26, 989–1001.
[5] Duncan, E.G., Maher, W.A., Foster, S.D., 2015. Contribution of arsenic species in unicellular algae to the cycling of arsenic in marine ecosystems. Environ Sci Technol 49, 33–50.
[6] Duncan, E.G., Maher, W.A., Foster, S.D., Krikowa, F., 2013. The influence of arsenate and phosphate exposure on arsenic uptake, metabolism and species formation in the marine phytoplankton *Dunaliella tertiolecta*. Mar Chem 157, 78–85.
[7] Eker-Develi, E., Kideys, A.E., Tugrul, S., 2006. Effect of nutrients on culture dynamics of marine phytoplankton. Aquat Sci 68, 28–39.

[8] Fayiga, A.O., Nwoke, O.C., 2016. Phosphate rock: origin, importance, environmental impacts, and future roles. Environ Rev (Ott, , Can) 24, 403–415.
[9] Garbinski, L.D., Rosen, B.P., Chen, J., 2019. Pathways of arsenic uptake and efflux. Environ Int 126, 585–597.
[10] Guillard, R.R., Ryther, J.H., 1962. Studies of marine planktonic diatoms. I. *Cyclotella nana* (Hustedt), and *Detonula confervacea* (Cleve Gran.). Can J Microbiol 8, 229–239.
[11] Hasegawa, H., Rahman, M.A., Kitahara, K., Itaya, Y., Maki, T., Ueda, K., 2010. Seasonal changes of arsenic speciation in lake waters in relation to eutrophication. Sci Total Environ 408, 1684–1690.
[12] Hashihama, F., Suwa, S., Kanda, J., Ehama, M., Sakuraba, R., Kinouchi, S., et al., 2019. Arsenate and microbial dynamics in different phosphorus regimes of the subtropical Pacific Ocean. Prog Oceanogr 176, 102115.
[13] Heil, C.A., Revilla, M., Glibert, P.M., Murasko, S., 2007. Nutrient quality drives differential phytoplankton community composition on the southwest Florida shelf. Limnol Oceanogr 52, 1067–1078.
[14] Hierro, A., Olias, M., Ketterer, M.E., Vaca, F., Borrego, J., Canovas, C.R., et al., 2014. Geochemical behavior of metals and metalloids in an estuary affected by acid mine drainage (AMD). Environ Sci Pollut Res 21, 2611–2627.
[15] Howard, A.G., Comber, S.D.W., Kifle, D., Antai, E.E., Purdie, D.A., 1995. Arsenic speciation and seasonal changes in nutrient availability and micro-plankton abundance in Southampton Water, U.K. Estuar, Coast Shelf Sci 40, 435–450.
[16] Huang, K., Zhuang, Y., Wang, Z., Ou, L., Cen, J., Lu, S., et al., 2021. Bioavailability of organic phosphorus compounds to the harmful dinoflagellate *Karenia mikimotoi*. Microorganisms 9, 1961.
[17] Hussain, M.M., Wang, J., Bibi, I., Shahid, M., Niazi, N.K., Iqbal, J., et al., 2021. Arsenic speciation and biotransformation pathways in the aquatic ecosystem: The significance of algae. J Hazard Mater 403, 124027.
[18] Kaise, T., Fujiwara, S., Tsuzuki, M., Sakurai, T., Saitoh, T., Mastubara, C., 1999. Accumulation of arsenic in a unicellular alga *Chlamydomonas reinhardtii*. Appl Organomet Chem 13, 107–111.
[19] Karadjova, I.B., Slaveykova, V.I., Tsalev, D.L., 2008. The biouptake and toxicity of arsenic species on the green microalga *Chlorella salina* in seawater. Aquat Toxicol 87, 264–271.
[20] Lavoie, M., Le Faucheur, S., Fortin, C., Campbell, P.G., 2009. Cadmium detoxification strategies in two phytoplankton species: metal binding by newly synthesized thiolated peptides and metal sequestration in granules. Aquat Toxicol 92, 65–75.
[21] Levy, J.L., Stauber, J.L., Adams, M.S., Maher, W.A., Kirby, J.K., Jolley, D.F., 2005. Toxicity, biotransformation, and mode of action of arsenic in two freshwater microalgae (*Chlorella* sp. and *Monoraphidium arcuatum*). Environ Toxicol Chem 24, 2630–2639.
[22] Li, M.Z., Li, L., Shi, X.G., Lin, L.X., Lin, S.J., 2015. Effects of phosphorus deficiency and adenosine 5 '-triphosphate (ATP) on growth and cell cycle of the dinoflagellate *Prorocentrum donghaiense*. Harmful Algae 47, 35–41.
[23] Lin, S., Litaker, R.W., Sunda, W.G., 2016. Phosphorus physiological ecology and molecular mechanisms in marine phytoplankton. J Phycol 52, 10–36.
[24] Liu, C.L., Place, A.R., Jagus, R., 2017. Use of antibiotics for maintenance of axenic cultures of *Amphidinium carterae* for the analysis of translation. Mar Drugs 15, 242–255.
[25] Lomas, M.W., Burke, A.L., Lomas, D.A., Bell, D.W., Shen, C., Dyhrman, S.T., et al., 2010. Sargasso Sea phosphorus biogeochemistry: an important role for dissolved organic phosphorus (DOP). Biogeosciences 7, 695–710.
[26] Lopez, P.J., Descles, J., Allen, A.E., Bowler, C., 2005. Prospects in diatom research. Curr Opin Biotechnol 16, 180–186.
[27] Ma, Q., Chen, L., Zhang, L., 2023. Effects of phosphate on the toxicity and bioaccumulation of arsenate in marine diatom *Skeletonema costatum*. Sci Total Environ 857, 159566.
[28] Ma, X., Johnson, K.B., Gu, B., Zhang, H., Li, G., Huang, X., et al., 2022. The in-situ release of algal bloom populations and the role of prokaryotic communities in their establishment and growth. Water Res 219, 118565.
[29] Miao, A.J., Hutchins, D.A., Yin, K., Fu, F.X., Harrison, P.J., Wang, W.X., 2006. Macronutrient and iron limitation of phytoplankton growth in Hong Kong coastal waters. Mar Ecol: Prog Ser 318, 141–152.
[30] Neff, J.M., 1997. Ecotoxicology of arsenic in the marine environment. Environ Toxicol Chem 16, 917–927.
[31] Ou, L., Qin, X., Shi, X., Feng, Q., Zhang, S., Lu, S., et al., 2020. Alkaline phosphatase activities and regulation in three harmful Prorocentrum species from the coastal waters of the East China Sea. Microb Ecol 79, 459–471.
[32] Ou, L.J., Huang, X.Y., Huang, B.Q., Qi, Y.Z., Lu, S.H., 2015. Growth and competition for different forms of organic phosphorus by the dinoflagellate *Prorocentrum donghaiense* with the dinoflagellate *Alexandrium catenella* and the diatom *Skeletonema costatum* s.l. Hydrobiologia 754, 29–41.
[33] Ou, L.J., Wang, D., Huang, B.Q., Hong, H.S., Qi, Y.Z., Lu, S.H., 2008. Comparative study of phosphorus strategies of three typical harmful algae in Chinese coastal waters. J Plankton Res 30, 1007–1017.
[34] Papry, R.I., Miah, S., Hasegawa, H., 2022. Integrated environmental factor-dependent growth and arsenic biotransformation by aquatic microalgae: a review. Chemosphere 303, 135164.
[35] Price, N.M., Harrison, G.I., Hering, J.G., Hudson, R.J., Nirel, P.M.V., Palenik, B., et al., 1989. Preparation and chemistry of the artificial algal culture medium Aquil. Biol Oceano 6, 443–461.
[36] Rahman, M.A., Hasegawa, H., 2012. Arsenic in freshwater systems: influence of eutrophication on occurrence, distribution, speciation, and bioaccumulation. Appl Geochem 27, 304–314.
[37] Ring, B., Wrighton, S.A., Mohutsky, M., 2014. Reversible mechanisms of enzyme inhibition and resulting clinical significance. In: Nagar, S., Argikar, U.A., Tweedie, D.J. (Eds.), Enzyme Kinetics in Drug Metabolism: Fundamentals and Applications. Humana Press, Totowa, NJ, pp. 37–56.
[38] Roesijadi, G., 1981. The significance of low-molecular weight, metallothionein-like proteins in marine invertebrates - current status. Mar Environ Res 4, 167–179.
[39] Sanders, J.G., Riedel, G.F., 1993. Trace element transformation during the development of an estuarine algal bloom. Estuaries 16, 521–532.
[40] Sanders, J.G., Windom, H.L., 1980. The uptake and reduction of arsenic species by marine algae. Estuar Coast Mar Sci 10, 555–567.
[41] Snow, J.T., Holdship, P., Rickaby, R.E.M., 2020. Antagonistic co-limitation through ion promiscuity - on the metal sensitivity of *Thalassiosira oceanica* under phosphorus stress. Sci Total Environ 699, 134080.
[42] Stoecker, D., Tillmann, U., Granéli, E., 2006. Phagotrophy in harmful algae. In: Granéli, E., Turner, J.T. (Eds.), Ecology of Harmful Algae. Springer Berlin Heidelberg, Berlin, Heidelberg, pp. 177–187.
[43] Tawfik, D.S., Viola, R.E., 2011. Arsenate replacing phosphate: alternative life chemistries and ion promiscuity. Biochemistry 50, 1128–1134.
[44] Wallace, W.G., Lee, B.G., Luoma, S.N., 2003. Subcellular compartmentalization of Cd and Zn in two bivalves. I. Significance of metal-sensitive fractions (MSF) and biologically detoxified metal (BDM). Mar Ecol: Prog Ser 249, 183–197.
[45] Wang, N.X., Li, Y., Deng, X.H., Miao, A.J., Ji, R., Yang, L.Y., 2013. Toxicity and bioaccumulation kinetics of arsenate in two freshwater green algae under different phosphate regimes. Water Res 47, 2497–2506.
[46] Wang, Y., Li, R.X., Dong, S.L., Li, Y., Sun, P., Wang, X.D., 2011. Relationship between cell volume and cell carbon and cell nitrogen for ten common dinoflagellates. Acta Ecol Sin 31, 6540–6550.
[47] Wang, Y., Wang, S., Xu, P.P., Liu, C., Liu, M.S., Wang, Y.L., et al., 2015. Review of arsenic speciation, toxicity and metabolism in microalgae. Rev. Environ. Sci Bio 14, 427–451.
[48] Wang, Y., Zhang, C., Zheng, Y., Ge, Y., 2017. Bioaccumulation kinetics of arsenite and arsenate in *Dunaliella salina* under different phosphate regimes. Environ Sci Pollut Res 24, 21213–21221.
[49] Wang, Y., Zheng, Y., Liu, C., Xu, P., Li, H., Lin, Q., et al., 2016. Arsenate toxicity and metabolism in the halotolerant microalga *Dunaliella salina* under various phosphate regimes. Environ Sci: Process Impacts 18, 735–743.
[50] Wang, Z., Gui, H., Luo, Z., Zhen, Z., Yan, C., Xing, B., 2019. Dissolved organic phosphorus enhances arsenate bioaccumulation and biotransformation in *Microcystis aeruginosa*. Environ Pollut 252, 1755–1763.
[51] Wang, Z., Luo, Z., Yan, C., Che, F., Yan, Y., 2014. Arsenic uptake and depuration kinetics in *Microcystis aeruginosa* under different phosphate regimes. J Hazard Mater 276, 393–399.
[52] Xu, J.Y., Li, H.B., Liang, S., Luo, J., Ma, L.Q., 2014. Arsenic enhanced plant growth and altered rhizosphere characteristics of hyperaccumulator *Pteris vittata*. Environ Pollut 194, 105–111.
[53] Xue, X.M., Ye, J., Raber, G., Rosen, B.P., Francesconi, K., Xiong, C., et al., 2019. Identification of steps in the pathway of arsenosugar biosynthesis. Environ Sci Technol 53, 634–641.
[54] Yan, C., Wang, Z., Luo, Z., 2014. Arsenic efflux from *Microcystis aeruginosa* under different phosphate regimes. PLoS One 9, e116099.
[55] Young, C.L., Ingall, E.D., 2010. Marine dissolved organic phosphorus composition: Insights from samples recovered using combined electrodialysis/reverse osmosis. Aquat Geochem 16, 563–574.
[56] Zhang, S.F., Yuan, C.J., Chen, Y., Chen, X.H., Li, D.X., Liu, J.L., et al., 2016. Comparative transcriptomic analysis reveals novel insights into the adaptive response of *Skeletonema costatum* to changing ambient phosphorus. Front Microbiol 7, 01476.
[57] Zhang, S.Y., Rensing, C., Zhu, Y.G., 2014. Cyanobacteria-mediated arsenic redox dynamics is regulated by phosphate in aquatic environments. Environ Sci Technol 48, 994–1000.
[58] Zhang, W., Huang, L., Wang, W.X., 2012. Biotransformation and detoxification of inorganic arsenic in a marine juvenile fish *Terapon jarbua* after waterborne and dietborne exposure. J Hazard Mater 221–222, 162–169.
[59] Zhang, X., Lin, S., Liu, D., 2020. Transcriptomic and physiological responses of *Skeletonema costatum* to ATP utilization. Environ Microbiol 22, 1861–1869.